arXiv:0712.0334v1 [physics.atom-ph] 3 Dec 2007

Retrieval of electron-atom scattering cross sections from laser-induced electron rescattering of atomic negative ions in intense laser fields

XiaoXin Zhou[1,2], Zhangjin Chen[1], Toru Morishita[1,3], Anh-Thu Le[1], and C. D. Lin[1]
[1] *J. R. Macdonald Laboratory, Physics Department,*
Kansas State University, Manhattan, Kansas 66506-2604 USA
[2] *College of Physics and Electronic Engineering, Northwest Normal University, Lanzhou 730070, P. R. China*
[3] *Department of Applied Physics and Chemistry, University of Electro-Communications, Tokyo, 182-8585,*
Japan and PRESTO, Japan Science and Technology Agency, Kawaguchi, Saitama, 332-0012, Japan
(Dated: February 2, 2008)

We investigated the two-dimensional electron momentum distributions of atomic negative ions in an intense laser field by solving the time-dependent Schr?dinger equation (TDSE) and using the first- and 2nd-order strong-field approximations (SFA). We showed that photoelectron energy distributions and low-energy photoelectron momentum spectra predicted from SFA are in reasonable agreement with the solutions from the TDSE. More importantly, we showed that accurate electron-atom elastic scattering cross sections can be retrieved directly from high-energy electron momentum spectra of atomic negative ions in the laser field. This opens up the possibility of measuring electron-atom and electron-molecule scattering cross sections from the photodetachment of atomic and molecular negative ions by intense short lasers, respectively, with temporal resolutions in the order of femtoseconds.

I. INTRODUCTION

In the past two decades, the energy and momentum spectra of electrons generated by the ionization of atoms or detachment of negative ions by intense laser pulses have been widely investigated [1, 2]. In particular, the detachment of negative hydrogen and fluorine ions in intense laser fields have been reported in experiments [3, 4, 5, 6, 7] and in theory [8, 9, 10, 11, 12, 13, 14], using either the strong-field approximation (SFA) or by solving the time-dependent Schr?dinger equation (TDSE). These studies have shown that experimentally observed spectra are largely well reproduced by theoretical calculations. However, the electrons measured in these experiments tend to be restricted to low energies, and SFA and TDSE calculations are often carried out by separate groups using different additional approximations.

In this paper, we studied the photodetachment of H^- and F^- negative ions in short intense laser pulses. Our goal is to examine the electron energy distributions and two-dimensional (2D) electron momentum spectra over a broad energy range, from the threshold up to 10 UP, where UP is the ponderomotive energy. We will use the standard first-order SFA (SFA1) and the second-order SFA (SFA2) to describe the photodetachment process, as well as obtaining the same spectra by solving the TDSE directly. The negative ion will be approximated by a model potential and the same potential is used in the SFA and TDSE calculations. We will establish, based on specific numerical results, the accuracy of the SFA for describing the photodetachment of negative ions by lasers. In SFA, it was assumed that electrons released into the continuum can be described as a free electron in the laser field, and that there are no excited states in the target atom. Both approximations are expected to work better for negative ion targets than for atomic targets. Indeed our calculations showed that the total electron energy spectra and the electron momentum spectra at low energies calculated from the SFA are in quite good overall agreement with the TDSE results, to within about a factor of two. Such agreement has not been seen if the targets are neutral atoms or positive ions [15]. Our major goal, however, is to establish that high-energy electron momentum spectra of negative ions induced by intense short laser pulses can be used to extract the elastic differential cross sections of neutral atoms by free electrons. Similar conclusions have been shown recently for atoms where electron-ion scattering cross sections can be extracted from laser-induced high-energy electron momentum spectra of neutral atoms [16].

In Section II, we summarize the theoretical models used. The numerical results for H^- and F^- from SFA and TDSE are presented and analyzed in Section III, for both the energy distributions and the 2D momentum distributions. From the high-energy 2D photoelectron momentum distributions we will extract the e-H and e-F elastic scattering cross sections. In Section IV we summarize the results and discuss the important possible applications of using laser-induced photoelectron spectra for probing time-resolved electron-atom or electron-molecule collisions. Atomic units are used throughout, unless otherwise indicated.

II. THEORETICAL METHODS

We will model each negative ion in the single-active electron (SAE) approximation. In this model, the time-dependent wavefunction of the active electron in the laser field is governed by

$$i\frac{\partial}{\partial t}\psi(\mathbf{r},t) = [H_0 + H'(t)]\psi(\mathbf{r},t) \tag{1}$$

where $H_0 = -\frac{1}{2}\nabla^2 + V(\mathbf{r})$ is the electron Hamiltonian of the laser-free system, with $V(\mathbf{r})$ being the atomic model potential, and $H'(t) = \mathbf{r}\cdot\mathbf{E}(t)$ is the interaction of the electron with the laser's electric field $\mathbf{E}(t)$. Equation (1) can be solved numerically by using the split-operator method [17, 18]. The electron momentum spectra are obtained by projecting out the final time-dependent wavefunction after the laser pulse is over using the continuum scattering eigenstates of the laser-free Hamiltonian. For electrons with momentum p in the direction $\hat{\mathbf{p}}$, with respect to the laser polarization direction, if the detachment amplitude is f, then the angular distributions at energy $E = p^2/2$ is given by

$$\frac{\partial P}{\partial \mathbf{p}} = |f(\mathbf{p})|^2. \tag{2}$$

This equation can also be rewritten in terms of 2D momentum distributions. By integrating over the directions of photoelectrons at a fixed energy E, the energy dependence of the photoelectrons are calculated from

$$\frac{\partial P}{\partial E} = \int |f(\mathbf{p})|^2 p d\hat{\mathbf{p}}. \tag{3}$$

In the strong-field approximation, the detachment probability of electrons with momentum $\mathbf{p}$ is expressed as [19]

$$f(\mathbf{p}) = f^{(1)} + f^{(2)} \tag{4}$$

where the first-order of SFA amplitude (SFA1) is

$$f^{(1)} = -i\int_{-\infty}^{\infty} dt \left\langle \chi_{\mathbf{p}}(t) \left| H'(t) \right| \Psi_0(t)\right\rangle \tag{5}$$

and the second-order of SFA amplitude (SFA2) is

$$\begin{aligned} f^{(2)} \;=\; & -\int_{-\infty}^{\infty} dt \int_{-\infty}^{t} dt' \int d\mathbf{k} \left\langle \chi_{\mathbf{p}}(t) \left| V \right| \chi_{\mathbf{k}}(t)\right\rangle \\ & \times \left\langle \chi_{\mathbf{k}}(t') \left| H'(t') \right| \Psi_0(t')\right\rangle \end{aligned} \tag{6}$$

Here $\chi_{\mathbf{p}}(t)$ and $\Psi_0(t')$ are the Volkov states of a continuum electron with momentum $\mathbf{p}$ and the initial state, respectively. The evaluation of the integral (6) has been discussed in [19]. In SFA2, we have used the saddle point approximation in evaluating the integration over $d\mathbf{k}$ where $\mathbf{k}$ is the momentum of photoelectron in the intermediate Volkov state. Otherwise all the integrals are evaluated numerically without additional approximations.

For the model potential, for H$^-$, we take it from [20]:

$$V(r) = -(1+\frac{1}{r})e^{-2r} - \frac{\alpha_d}{2r^4}(1-e^{(r/r_c)^6}) + V_0(r) \tag{7}$$

where $V_0(r) = (c_0 + c_1 r + c_2 r^2)e^{-\beta r}$.

Note that the polarization of the core (H atom) has been included in (7), with α_d and r_c being the polarizability and the cutoff constant, respectively. The parameters in (7) are listed in Ref. [20]. For the negative fluorine ion, we chose the potential to have the form,

$$V(r) = -a_1\frac{e^{-\alpha_1 r}}{r} - a_2\frac{e^{-\alpha_2 r}}{r}. \tag{8}$$

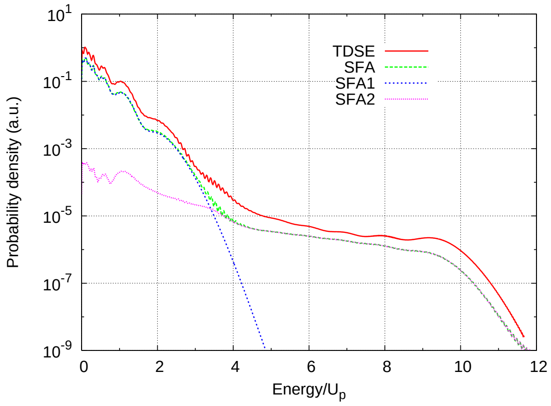

FIG. 1: (Color online) Energy spectra of laser-induced photoelectrons of H$^-$ obtained from TDSE (red solid line) and from SFA (green dotted line). The laser parameters are $I = 1.0 \times 10^{11}$ W/cm^2 and $\lambda = 10600$ nm for a pulse with 3 optical cycles (see text).

From fitting, the parameters a_1, a_2, α_1 and α_2 obtained are 5.137, 3.863, 1.288 and 3.545 respectively. This potential gives the correct ground state energy of the negative fluorine ion, and its lowest p-orbital eigenfunction agrees well with the tabulated Hartree-Fock wavefunction for F$^-$.

III. RESULTS AND DISCUSSION

We used the TDSE and SFA to calculate the energy spectra and the 2D momentum distributions of H$^-$ and F$^-$ in intense laser fields. For H$^-$, we took peak laser intensity of $I = 1.0\times10^{11}$ W/cm^2, wavelength $\lambda = 10600$ nm and pulse duration of 3 cycles. The electric field has the form $E(t) = E_0 F(t)\cos(\omega t + \phi)$ where ϕ (we chose it to be zero) is the carrier envelope phase, and $F(t) = \cos^2(\pi t/\tau)$ where $\tau = 3T$ ($|t| \leq \tau/2$), with T being the period of the laser. For this laser pulse, the ponderomotive energy is 1.05 eV, and it needs 16 photons ($\hbar\omega = 0.117$ eV) to remove the electron from H$^-$. The Keldysh parameter is 0.6, thus the electron detachment is well in the tunnelling regime.

In Fig. 1 we show the calculated energy spectra of the detached photoelectrons where the energy is expressed in units of U_p. In the SFA, the low-energy part below about 3.5 U_p is dominated by SFA1, while the yield above $4U_p$ is dominated almost entirely by SFA2, i.e., it is due to the recollision between the detached electrons with the neutral target H. The figure also shows that the energy spectra obtained from SFA are only about a factor of two smaller than those obtained from the TDSE. For neutral atom or positive ion targets the absolute total ionization yields calculated using SFA are generally much smaller, close to one order or more smaller than those obtained from TDSE [15].

Fig. 2 shows the 2D momentum distributions of the

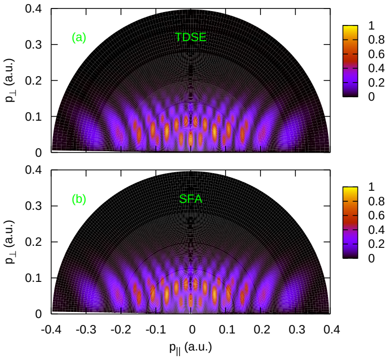

FIG. 2: (Color online) 2D momentum distributions of laser-induced photoelectrons of H$^-$ in the low energy region, obtained from TDSE (a) and from SFA (b). The horizontal axis is the electron momentum along the direction of laser polarization and the vertical axis is any axis perpendicular to it (the electron spectrum has cylindrical symmetry.) The laser parameters are the same as in Fig. 1.

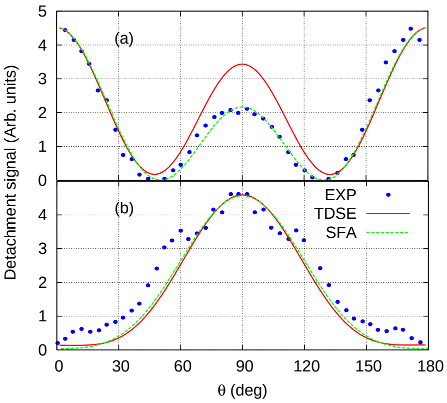

FIG. 3: (Color online) Angular distributions of laser-induced photoelectrons of H$^-$, generated by a laser with (a) wavelengh $\lambda = 2150$ nm, intensity $I = 1.3 \times 10^{11}$ W/cm^2, for electron energy $E = 0.34$ eV; (b) for intensity $I = 6.5 \times 10^{11}$ W/cm^2, and electron energy $E = 0.12$ eV. The TDSE and SFA results are compared to the experimental data of Ref. [3].

detached electrons at low energies where $p_{||}$ refers to the direction of the laser polarization and $p_\perp = \sqrt{p^2 - p_{||}^2}$ is perpendicular to it. We normalized the data to the same peak value in the two graphs. There are several special features that should be mentioned. First, the 2D spectra predicted from SFA1 and from TDSE are very close to each other. Second, the 2D spectra exhibit clean structures that may be attributed to multiphoton detachment (MPD), despite that it is in the tunneling regime. It is interesting to compare these low-energy 2D momentum spectra with those from neutral atomic targets [17]. To begin with, for atomic targets, the low-energy momentum spectra show fan-like structure emanating from the origin. These fan-like structures have been observed experimentally [21, 22], and are seen only from the TDSE calculations, not from the SFA1 calculations. The fan-like structures had been attributed to the long-range Coulomb interaction between the electron and the positive atomic ion after the atom is ionized by the laser [17, 23]. For negative ion targets, there is no long-range Coulomb interaction between the electron and the neutral atom following the detachment of the electron by the laser, thus the fan-like structure is absent in the TDSE results, as shown in Fig. 2(a). Figs. 2(a) and (b) both show clear MPD peaks. The angular distribution of the lowest MPD peak has a maximum at 90° (even parity), thus the dominant angular momentum quantum number should be even. For atomic targets, the dominant angular momentum of the photoelectrons at low energies can be calculated from the propensity rule given in Chen *et al.* [17]. Since the minimum number of photons needed to remove the electron at the laser intensity used is 16 and that the ground state of H? is an s-orbital, Fig. 8 of Chen *et al.* [17] shows that the dominant angular momentum is six, and thus the parity is even, in agreement with the calculated results shown in Fig. 2. Note that the next MPD peak would have odd parity since one more photon is absorbed, as clearly seen from the calculated spectra.

Low-energy photoelectron angular distributions of H$^-$ have been reported by Reichle *et al.* [3] using lasers with $\lambda = 2150$ nm ($\hbar\omega = 0.576$ eV), pulse duration (FWHM) of 250 fs, at two peak intensities $I = 1.3 \times 10^{11}$ W/cm^2 and $I = 6.5 \times 10^{11}$ W/cm^2, corresponding to Keldysh parameters of 2.6 and 1.2, respectively. Unlike the previous example, this is in the multiphoton regime. In fact, the first low-energy photoelectron peak can be attributed to two-photon absorption. In Fig. 3 we show the angular distributions for photoelectron energy at 0.34eV for $I = 1.3 \times 10^{11}$ W/cm^2 and at 0.12 eV for $I = 6.5 \times 10^{11}$ W/cm^2. We compare the experimental data with SFA1 and with TDSE calculations. Both the SFA1 and the TDSE results agree well with the experimental results [the actual values from SFA1 shown have been scaled to agree with the TDSE results at small angles in (a) and at 90° in (b)]. Note that it appears that the SFA1 results are in better agreement with the experimental data in Fig. 3(a) than the TDSE results. However, the volume effect is not included in our calculations and we considered the agreement satisfactory. Our calculations also showed that the angular distributions are independent of the pulse durations.

Next we return to the laser parameters used in Figs. 1 and 2, and study the 2D momentum distributions of the detached electrons in the high energy region. It is well known that these high energy electrons are generated by the rescattering processes. In order to highlight these high-energy features, in Figs. 4(a) and 4(b) we show the 2D momentum distributions by renormalizing them such that the total ionization probability density at each energy is the same. The results from the TDSE and from SFA appear to be quite similar globally. Here we focus on the outermost ring of the 2D spectra. The distribu-

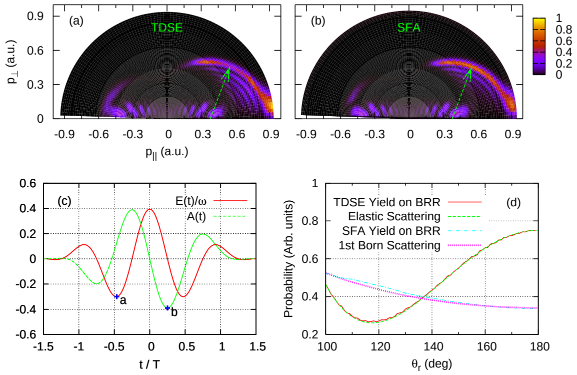

FIG. 4: (Color online) (a,b): 2D momentum distributions of laser-induced photoelectrons for H$^-$ in the high energy region, obtained from TDSE and SFA, respectively; (c) The electric field and the vector potential of the 3-cycle pulse are depicted, indicating the "born time" of the detached electron and its return time;(d) Elastic scattering cross sections extracted along the BRR from the TDSE calculations (red solid line), and are compared to the electron-H scattering cross sections (green dotted lines). Also shown are the corresponding results from SFA and from FBA.

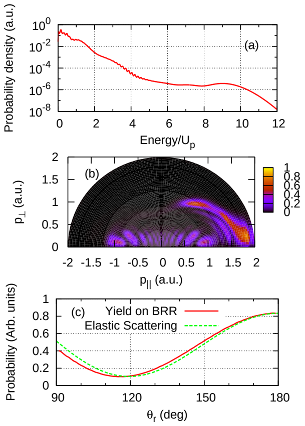

FIG. 5: (Color online) (a) Energy spectra of laser-induced photoelectrons of F$^-$ obtained from solving the TDSE. The laser parameters are $I = 1.3 \times 10^{13}$ W/cm^2 and $\lambda = 1800$ nm for a pulse with 3 optical cycles; (b) 2D electron momentum distributions in the high energy region; (c) Elastic scattering cross sections, extracted along the BRR from the TDSE (red solid line) calculation, as compared to the e-F elastic scattering cross sections (green dotted line).

tions along this ring have been studied for laser-generated photoelectrons from neutral atoms recently [16]. They are called back rescattered ridge (BRR) electrons, representing returning electrons that have been rescattered into the backward directions by the target ion. The BRR electrons in Fig. 4(a) or 4(b) are electrons that have been rescattered into the backward directions by the neutral atomic hydrogen. In Fig. 4(c), we depict the electric field and the vector potential of a three-cycle laser pulse used in the calculation. Electrons that are released at the half-cycle centered at "a" [see Fig. 4(c)] will return near "b", with peak kinetic energy at $p_r^2/2 = 3.17\bar{U}_p$ where $\bar{U}_p = A_r^2/4$, with A_r being the vector potential at "b". An electron that is scattered into the backward direction with momentum $p_r\hat{\mathbf{p}}_r$ at "b" will gain additional momentum A_r as it emerges from the laser field. Thus the momentum of the BRR electrons at the end of the laser pulse is given by $\mathbf{p} = -\mathbf{A}_r + \mathbf{p}_r$, or $p_{||} = -A_r - p_r \cos\theta_r$ and $p_\perp = p_r \sin\theta_r$, where $p_r = 1.26A_r$. Here θ_r is the scattering angle measured from the "incident" direction of the recolliding electrons and for BRR, we consider θ_r larger than only. (The BRR ring is indicated by showing an arrow with length from its shifted center in Figs. 4(a) and 4(b).) In Fig. 4(d) we show the yield of the photoelectrons along the BRR, plotted against the scattering angle θ_r. On the same graph we also show the differential elastic cross sections of electrons scattered by atomic hydrogen. For the laser parameters used in this example, $A_r = 0.39$ and thus the electron's kinetic energy is $p_r^2 = 3.28$ eV. In Fig. 4(d), the yields along the BRR obtained from the TDSE calculations are compared to "exact" electron-hydrogen differential scattering cross sections (normalized), and they are in good agreement. On the same graph, the yields from the SFA2 calculations are compared to the differential elastic e-H scattering cross sections calculated in the first Born approximation (FBA) and they also show good agreement between them. In the SFA2, the returning electron interacts with the H atom only once and thus the elastic scattering cross section is given by the FBA. The yields along the BRR obtained from the TDSE solution and from SFA2 are clearly different. In particular, the extracted elastic differential cross section from TDSE shows a minimum and becomes larger at large angles. The one extracted from SFA2 or from FBA show that the differential cross sections decrease monotonically with increasing angles. We thus confirm that one can extract differential elastic e-H scattering cross sections in the backward directions from laser-induced photodetachment of H? ions by intense short laser pulses.

We have carried out similar studies for F$^-$ ions, using a 3-cycle laser pulse with wavelength $\lambda = 1800$ nm and peak intensity $I = 1.3 \times 10^{13}$ W/cm^2. The ponderomotive energy U_p is 3.93 eV. In this case, it needs 11 photons to remove the electron from F$^-$. We show the energy spectra of the detached electron from F$^-$ ions in Fig. 5(a). In Fig. 5(b), we show the 2D momentum distributions of the detached electrons for F$^-$ calculated using TDSE, and focusing on electrons along the BRR. The yields along the BRR show a clear minimum. This minimum is due to the minimum in the differential scattering cross sections between the electrons and neutral fluorine atoms. For the laser parameters used, we calculated that the returning electron energy is 11.8 eV. In Fig. 5(c) we show extracted differential scattering cross sections from laser-induced momentum distributions along the BRR, and compare the results with the calculated elastic e-F scattering cross sections. The good agreement between the two demonstrates once again that one can extract electron-atom scattering cross sections from laser-induced photoelectron momentum distributions of negative ions.

IV. SUMMARY AND PERSPECTIVE

In this paper we studied the photodetachment cross sections of atomic negative ions by an intense laser pulse, using the first-order and second-order strong-field approximations (SFA1+ SFA2), and by solving the time-dependent Schr?dinger equation (TDSE) directly. We established that the electron energy distributions and the 2D electron momentum distributions obtained from SFA and from TDSE are quite close to each other. On the other hand, there are important differences in the 2D electron momentum distributions at high energies. These electrons are identified to be distributed along the so-called back rescattered ridge (BRR). From the 2D momentum distributions along the BRR, we showed that elastic scattering cross sections between free electrons with neutral atom targets can be accurately extracted. In other words, we have shown that specific structure information which has previously been probed with electron scattering can also be obtained from the photodetachment of the negative ions by short intense laser pulses.

The results from this work have two important implications. Since the laser pulses have short durations down to a few femtoseconds, the present results imply that one can probe the time-evolution of a transient negative ion system using this method, similar to what one can do with neutral targets [16, 24]. Second, it shows that one can extract electron-atom or electron-molecule scattering cross sections by carrying out photodetachment measurements of their negative ions with intense laser pulses. One can control the electron scattering energies by changing laser's intensity or wavelength. For many atomic and molecular species, including radicals, it may be easier to produce or control their negative ions than their neutrals. In this case photodetachment of negative ions by intense short laser pulses can potentially offer a much better means for measuring electron scattering cross sections.

Although we have carried out calculations using negative atomic ions treated by a model potential, we believe that our conclusions applies to real many-electron atomic and molecular systems. In fact, it is well-known that electron scattering off an atom or molecule cannot be accurately described using a simple model potential at low incident energies. At present, it is not possible to obtain accurate 2D momentum spectra for many-electron atoms or molecules from TDSE. If accurate laser-generated electron spectra are available, one would expect the data to reveal many-electron effects. For example, in electron-hydrogen atom scattering, in Fig. 4d we show that the differential cross section has a minimum at 120° according to the model potential we have used. Experimental data by Williams [25] at $E = 3.4$ eV indicated that the minimum occurs closer to about 80° (At 8.7 eV the minimum is at about 115°). To achieve agreement for electron scattering at such low energies, more advanced theoretical models which treats both electrons together, such as the Kohn variational principle [26], the polarized orbital method [27] or close-coupling methods [28] are needed. It remains to be seen if laser-induced photoelectron spectra can measured with high precision such that many-electron effects are revealed. Unlike electron scattering which is a linear phenomenon, laser-induced photoelectron yields are nonlinear phenomena. On the other hand, the present paper shows that the extracted electron scattering cross sections from the BRR are independent of the laser parameters, including their intensity or wavelength (and the duration [19]), so long that the returning electron has the same energy. This may provide an added check on the electron scattering cross sections extracted from laser-induced photoelectron measurements.

Acknowledgments

This work was supported in part by Chemical Sciences, Geosciences and Biosciences Division, Office of Basic Energy Science, US Department of Energy. X. X. Zhou was supported in part by the National Natural Science Foundation of China (Grant No. 10674112). TM was supported in part by the PRESTO program of the Japan Science and Technology Agency (JST), by a Grants-in-Aid for Scientific Research from a Japanese Society for the Promotion of Science (JSPS), by the 21st Century COE program on "Coherent Optical Science", and by JSPS Bilateral joint program between US and Japan.

[1] D. B. Milošević, G. G. Paulus, D. Bauer and W. Becker, J. Phys. B **39**, R203 (2006).
[2] P. Agostini and L. F. DiMauro, Rep. Prog. Phys. **67**, 813 (2004).
[3] R. Reichle, H. Helm and I. Y. Kiyan, Phys. Rev. Lett. **87**, 243001 (2001).
[4] R. Reichle, H. Helm, and I. Y. Kiyan, Phys. Rev. A **68**, 063404 (2003).
[5] I. Y. Kiyan and H. Helm, Phys. Rev. Lett. **90**, 183001 (2003).
[6] B. Bergues, Y. Ni, H. Helm, and I. Y. Kiyan, Phys. Rev. Lett. **95**, 263002 (2005).
[7] B. Bergues, Z. Ansari, D. Hanstorp, and I. Y. Kiyan, Phys. Rev. A **75**, 063415 (2007).
[8] D. B. Milošević, A. Gazibegovic-Busuladzic, and W. Becker, Phys. Rev. A **68**, 050702 (2003).
[9] A. Gazibegovic-Busuladzic, D. B. Milošević, and W. Becker,PRA **70**, 053403 (2004).

[10] S. Bivona, G. Bonanno, R. Burlon, and C. Leone, Phys. Rev. A **76**, 021401(R) (2007).

[11] H. R. Reiss, Phys. Rev. A **76**, 033404 (2007).

[12] M. V. Frolov, N. L. Manakov, E. A. Pronin, and A. F. Starace, Phys. Rev. Lett. **91**, 053003 (2003).

[13] K. Krajewska, II. I. Fabrikant, and A. F. Starace, Phys. Rev. A **74**, 053407 (2006).

[14] C. Arendt, D. Dimitrovski, and J. Briggs, Phys. Rev. A **76**, 023423(2007).

[15] C. C. Chirila and R. M. Potvliege, Phys. Rev. A **71**, 021402 (2005).

[16] T. Morishita, A. T. Le, Z. Chen and C. D. Lin, Phys. Rev. Lett. in press (2007).

[17] Z. Chen, T. Morishita, A. T. Le, M. Wickenhauser, X. M. Tong, and C. D. Lin, Phys. Rev. A **74**, 053405 (2006).

[18] T. Morishita, Z. Chen, S. Watanabe, and C. D. Lin, Phys. Rev. A **75**, 023407(2007).

[19] Z. Chen, T. Morishita, A. T. Le, and C. D. Lin, Phys. Rev. A **76**, 043402 (2007).

[20] C. Laughlin and S. I. Chu, Phys. Rev. A **48**, 4654(1993).

[21] C. M. Maharjan, A. S. Alnaser, I. Litvinyuk, P. Ranitovic, and C. L. Cocke, J. Phys. B **39**, 1955 (2006).

[22] A. Rudenko, K. Zrost, C. D. Schr?ter, V. L. B. de Jesus, B. Feuerstein, R. Moshammer, and J. Ullrich, J. Phys. B **37**, L407 (2004).

[23] D. G. Arbó, S. Yoshida, E. Persson, K. I. Dimitriou, and J. Burgdörfer, Phys. Rev. Lett. **96**, 143003 (2006).

[24] T. Morishita, A. T. Le, Z. Chen, and C. D. Lin, New J. Phys. in press (2007).

[25] J. F. Williams, J. Phys. B **8**, 1683 (1975).

[26] C. Schwartz, Phys. Rev. **121**, 788 (1961).

[27] A. Temkin, Phys. Rev. **126**, 130 (1962).

[28] P. G. Burke, D. F. Gallaher and S. Geltman, J. Phys. B **2**, 1142 (1969).